COMPDYN 2009
ECCOMAS Thematic Conference on
Computational Methods in Structural Dynamics and Earthquake Engineering
M. Papadrakakis, N.D. Lagaros, M. Fragiadakis (eds.)
Rhodes, Greece, 22-24 June 2009

DYNAMIC FINITE DEFORMATION VISCOELASTICITY IN PRINCIPAL STRETCHES: ENERGY-CONSISTENT TIME INTEGRATION USING MIXED FINITE ELEMENTS

Melanie Müller[1], **Michael Groß**[2] **and Peter Betsch**[2]

[1]University of Siegen
Paul-Bonatz Str. 9-11, 57068 Siegen
e-mail: mueller@imr.mb.uni-siegen.de

[2] University of Siegen
Paul-Bonatz Str. 9-11, 57068 Siegen
e-mail: {gross, betsch}@imr.mb.uni-siegen.de

Keywords: viscoelasticity, Ogden material model, principal stretches, enhanced assumed strain elements, discrete gradient, fulfillment of energy balance

Abstract. *The main goal of the present work is to describe viscoelastic isotropic material behaviour with an internal variable, which is derived from the well-known stretch tensor U. Furthermore it is shown a time integration method, which fulfills the underlying balances of the system. The discretisation in space is performed by the enhanced assumed strain (EAS) elements, which remedy the locking effects of the nonlinear displacement based elements. The chosen material model is the Ogden material model. This model depends merely on principal stretches. The theory is confirmed by two examples of a free flying L.*

1 INTRODUCTION

The numerical implementation of the concept of internal variables for viscoelastic material is increasingly performed only since [1]. A further development of this approach was done by [2, 3, 4]. These papers deal with numerical simulations for isothermal processes. In [5] was developed a concrete model with a multiplicative decomposition of the deformation gradient in an elastic and inelastic part. This decomposition is motivated by the transient network theory. A further work on this micromechanical level was done in [6]. Here in the level of continuum mechanics a fictive intermediate configuration is described. This configuration can be interpreted as a real existing intermediate configuration on molecular level. The usage of the internal variable $\mathcal{U}_i$ is motivated by [7]. For isotropic materials the invariants of the elastic strain measure $\mathcal{C}_e$, using $\mathcal{C}_i$ or $\mathcal{U}_i$, are the same.

The approach of the multiplicative split is also used in one of the newest works [8], which deals with viscoelastic materials in dynamics. Therein an internal variable $\mathcal{C}_i$ is used, which is derived by the right Cauchy-Green strain tensor for isotropic material behaviour. Moreover, the conservation properties are fulfilled up to the underlying tolerance of the Newton-Raphson iteration of the system. This leads to an enhanced numerical stability. The conservation properties are already mentioned in [9] and the references therein. This papers confirm the necessity of algorithmic conservation properties. The discretisation in time leads back to the discrete gradient of [10].

The well-known EAS elements for the spatial discretisation are derived by the Hu-Washizu functional which is mentioned in the works [11, 12]. These elements remedy the locking effect of the nonlinear standard displacement based elements. A great advantage for high Poissons number (rubberlike materials) in combination with high dominance of bending. A disadvantage is the instability under pressure loads, compare [13].

The Ogden model as material model is well-suited for rubberlike material. The main advantage of the Ogden material model is, that it can be well adapted to experimental data, see [14, 15]. According to [16], plastics, like rubbers become more and more important in the class of technical materials. This model depends only on principal stretches. A very compact illustration of the principal stretches in conjunction with quasi-incompressible elasticity include [17].

2 KINEMATICS

In order to describe a motion of a continuum a reference configuration in the domain $\mathcal{B}_0$ and a current configuration in the domain $\mathcal{B}_t$, is necessary. The continuum $\mathcal{B}$ can therefore be specified at the time $t = 0$ and an arbitrary time t. Figure 1 shows the correlation between both configurations.

The nonlinear mapping $\boldsymbol{\phi}$ transforms the configurations into each other. Whereby this mapping corresponds at the time $t = 0$ to the configuration vector $\mathbf{X}$ and at an arbitrary time point $t > 0$ to the current configuration vector

$$\mathbf{x} = \boldsymbol{\phi}(\mathbf{X}, t) \tag{1}$$

A further nonlinear mapping is given by $\boldsymbol{\phi}_\alpha$, which is necessary for the subsequent discretisation. The enhanced degrees of freedom $\mathbf{x}_\alpha$ are introduced analogously to the configuration vector $\mathbf{x}$:

$$\mathbf{x}_\alpha = \boldsymbol{\phi}_\alpha(\mathbf{X}_\alpha, t) \tag{2}$$

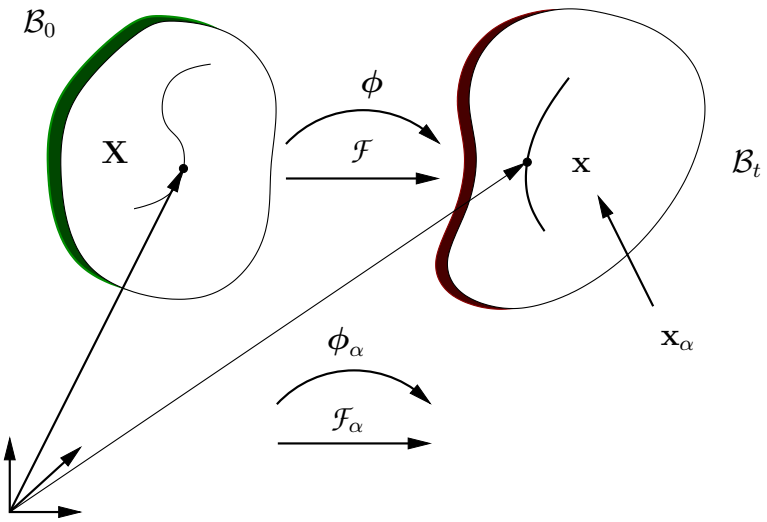

Figure 1: Reference and current configuration.

2.1 Deformations

The deformation of curves of a continuum during a motion leads to the deformation gradient $\mathcal{F}$. This deformation tensor expresses a linear correlation between the tangent vector of the reference and current configuration ($\mathbf{T}$, $\mathbf{t}$). The deformation gradient

$$\mathcal{F} = \frac{\partial \boldsymbol{\phi}}{\partial \mathbf{X}} = \frac{\partial \mathbf{x}}{\partial \mathbf{X}} \tag{3}$$

can be decomposed into a purely rotation tensor $\mathcal{R}$ and a purely stretch tensor $\mathcal{U}$:

$$\mathcal{F} = \mathcal{R}\,\mathcal{U} \tag{4}$$

Analogously to the deformation of curves, one gets linear correlations for surfaces ($\mathbf{A}$, $\mathbf{a}$) and volumes (V, v) with the cofactor $\operatorname{cof}\mathcal{F}$ and the Jacobian determinant J of the deformation gradient:

$$\operatorname{cof}\mathcal{F} = J\,\mathcal{F}^{-1} \qquad\qquad J = \det\mathcal{F} \tag{5}$$

The enhanced degrees of freedom $\mathbf{x}_\alpha$ lead to a deformation gradient of the enhanced degrees of freedom

$$\mathcal{F}_\alpha = \frac{\partial \boldsymbol{\phi}_\alpha}{\partial \mathbf{X}} = \frac{\partial \mathbf{x}_\alpha}{\partial \mathbf{X}} \tag{6}$$

which is included for the description of the whole deformation. The total deformation gradient is then called the enhanced deformation gradient

$$\mathcal{F}^{enh} = \mathcal{F} + \mathcal{F}_\alpha \tag{7}$$

2.2 Strains

The deformation gradient $\mathcal{F}$ yields the right Cauchy-Green strain tensor $\mathcal{C}$ in the domain $\mathcal{B}_0$ and the left Cauchy-Green strain tensor $\mathcal{b}$ in the domain $\mathcal{B}_t$:

$$\mathcal{C} = \mathcal{F}^{\mathrm{T}}\,\mathcal{F} \qquad\qquad \mathcal{b} = \mathcal{F}\,\mathcal{F}^{\mathrm{T}} \tag{8}$$

Another strain measure is the Lagrange strain tensor $\mathcal{E}$ which is formed by the right Cauchy-Green strain tensor $\mathcal{C}$ and the unit tensor I:

$$\mathcal{E} = \frac{1}{2}\left(\mathcal{C} - \mathit{I}\right) \tag{9}$$

The strains with the enhanced degrees of freedom are given by the right Cauchy-Green strain tensor

$$\mathcal{C}^{enh} = \mathcal{F}^{enh^{\mathrm{T}}}\,\mathcal{F}^{enh} \tag{10}$$

and the Lagrange strain tensor

$$\mathcal{E}^{enh} = \frac{1}{2}\left(\mathcal{C}^{enh} - \mathit{I}\right) \tag{11}$$

2.3 Principal stretches

The handling with principal stretches is described in [17]. The spectral decomposition of the right and left Cauchy-Green strain tensor is given by:

$$\mathcal{C} = \sum_{a=1}^{3} \bar{\lambda}_a\, \mathbf{N}^a \otimes \mathbf{N}^a \qquad\qquad \mathcal{b} = \sum_{a=1}^{3} \bar{\lambda}_a\, \mathbf{n}^a \otimes \mathbf{n}^a \tag{12}$$

with the eigenvalues $\bar{\lambda}_a$ and the eigenvectors $\mathbf{N}^a$ and $\mathbf{n}^a$, which are unit vector ($||\mathbf{N}^a|| = ||\mathbf{n}^a|| = 1$). The deformation gradient $\mathcal{F}$ can be described by the principal stretches λ_a ($a = 1,\, 2,\, 3$) and the normalised eigenvectors $\mathbf{n}^a$ and $\mathbf{N}^a$ of the tensors $\mathcal{b}$ and $\mathcal{C}$:

$$\mathcal{F} = \sum_{a=1}^{3} \lambda_a\, \mathbf{n}^a \otimes \mathbf{N}^a \tag{13}$$

The eigenvalues $\bar{\lambda}_a$ are associated with the principal stretches λ_a:

$$\bar{\lambda}_a = \lambda_a^2 \tag{14}$$

This leads to the expression of the right Cauchy-Green strain tensor:

$$\mathcal{C} = \sum_{a=1}^{3} \lambda_a^2\, \mathbf{N}^a \otimes \mathbf{N}^a \tag{15}$$

with $\lambda_a^2 > 0$. The derivatives of the eigenvalues with respect to the principal stretches and vice versa are defined as:

$$\begin{aligned} \frac{\partial \bar{\lambda}_a}{\partial \lambda_a} &= 2\,\lambda_a \\ \frac{\partial \lambda_a}{\partial \bar{\lambda}_a} &= \frac{1}{2}\,\bar{\lambda}_a^{-\frac{1}{2}} = \frac{1}{2\,\lambda_a} \end{aligned} \tag{16}$$

The eigenvectors $\mathbf{N}^a$ can be calculated by the eigenvalue problem

$$\left(\mathcal{C} - \lambda_a^2\, \mathit{I}\right) \mathbf{N}^a = \mathbf{0} \tag{17}$$

and the principal stretches λ_a can be derived by the corresponding characteristical polynomial

$$p(\lambda_a^2) := -\lambda_a^6 + I_1\,\lambda_a^4 - I_2\,\lambda_a^2 + I_3 = 0 \tag{18}$$

whereby the Invariants $I_1,\ I_2,\ I_3$ can be expressed by the principal stretches themselves:

$$\begin{aligned} I_1 &= \operatorname{tr} \mathcal{C} = \lambda_1^2 + \lambda_2^2 + \lambda_3^2 \\ I_2 &= \frac{1}{2}\,(I_1^2 - \operatorname{tr} \mathcal{C}^2) = \lambda_1^2\,\lambda_2^2 + \lambda_1^2\,\lambda_3^2 + \lambda_2^2\,\lambda_3^2 \\ I_3 &= \det \mathcal{C} = J^2 = \lambda_1^2\,\lambda_2^2\,\lambda_3^2 \end{aligned} \tag{19}$$

The derivatives of the principal stretches with respect to the right Cauchy-Green strain tensor vary in three cases. In the first case, all principal stretches are different $\lambda_1 \neq \lambda_2 \neq \lambda_3$:

$$\frac{\partial \lambda_a}{\partial \mathcal{C}} = \frac{1}{2}\,\lambda_a\,\mathcal{M}^a \tag{20}$$

If two of the three principal stretches are different $\lambda_1 = \lambda_2 \neq \lambda_3$, the derivative follows as:

$$\frac{\partial \lambda_1}{\partial \mathcal{C}} = \frac{1}{2}\,\lambda_1\,(\mathcal{C}^{-1} - \mathcal{M}^3) \qquad\qquad \frac{\partial \lambda_3}{\partial \mathcal{C}} = \frac{1}{2}\,\lambda_3\,\mathcal{M}^3 \tag{21}$$

In the last possibility, all principal stretches are the same $\lambda_1 = \lambda_2 = \lambda_3$:

$$\frac{\partial \lambda_1}{\partial \mathcal{C}} = \frac{1}{2}\,\lambda_1\,\mathcal{C}^{-1} \tag{22}$$

whereby the tensor $\mathcal{M}^a$ is defined as:

$$\mathcal{M}^a = \lambda_a^{-2}\,\mathbf{N}^a \otimes \mathbf{N}^a \tag{23}$$

The depicted equations in this subsection can be transfered to the notation with the enhanced degrees of freedom. The right Cauchy-Green strain tensor $\mathcal{C}^{enh}$ can be decomposed analogously:

$$\mathcal{C}^{enh} = \sum_{a=1}^{3} (\lambda_a^{enh})^2\,\mathbf{N}^{enh^a} \otimes \mathbf{N}^{enh^a} \tag{24}$$

In the following we deal exclusively with the right Cauchy-Green strain tensor $\mathcal{C}$ since we need the enhanced degrees of freedom solely for the discretisation.

2.4 Internal variable

The formulation of vicoelastodynamics is based on the concept of internal variables. There exist two groups of variables. On the one hand, we have the external variables, which are measureable and achievable. On the other hand, there are the internal variables, which are history dependend but not measurable. In the case of isotropic material one gets the current fictive dynamic state with both variables:

$$(\mathcal{C},\ \mathcal{U}_i) \tag{25}$$

In this connection, the right Cauchy-Green strain tensor $\mathcal{C}$ plays the role of the external variable and the viscous stretch tensor $\mathcal{U}_i$ is the internal variable. This definition leads to a symmetric strain tensor $\mathcal{C}_e$ (compare [7]):

$$\mathcal{C}_e = \mathcal{U}_i^{-1}\,\mathcal{C}\,\mathcal{U}_i^{-1} \tag{26}$$

3 FREE ENERGY FUNCTION

The isotropic free energy function ψ of a continuum is split into an elastic and a viscous part, see e.g. [6]. While the elastic part ψ_{ela} is merely dependend on the right Cauchy-Green strain tensor $\mathcal{C}$, the viscous part of the isotropic free energy function ψ_{vis} depends on the strain tensor $\mathcal{C}_e$:

$$\psi = \psi_{ela}(\mathcal{C}) + \psi_{vis}(\mathcal{C}_e) \tag{27}$$

Alternatively the isotropic free energy function can be described in the principal stretches:

$$\psi = \psi_{ela}(\lambda_a) + \psi_{vis}(\lambda_{e_a}) \tag{28}$$

Whereby λ_a ($a = 1,\ 2,\ 3$) are the well-known principal stretches of $\mathcal{C}$ and λ_{e_a} ($a = 1,\ 2,\ 3$) are the principal stretches of the tensor $\mathcal{C}_e$.

3.1 Ogden model

As material model for viscoelastodynamics we choose the Ogden material model. This model is merely written in dependence of the principal stretches. The advantage of the Ogden model is, that it can be easily fitted to experimental data (see [14, 15]). The free energy function for the elastic and viscous part is:

$$\begin{aligned}
\psi_{ela}(\lambda_a) &= \sum_{r=1}^{n} \frac{\mu_r}{\alpha_r} \left(\sum_{a=1}^{n_{dim}} \lambda_a^{\alpha_r} - n_{dim}\right) + \frac{\lambda}{4}\left(J^2 - 1 - 2\,\ln J\right) - \sum_{r=1}^{n} \mu_r\,\ln J \\
\psi_{vis}(\lambda_{e_a}) &= \sum_{r=1}^{n} \frac{\mu_{vis_r}}{\alpha_{vis_r}} \left(\sum_{a=1}^{n_{dim}} \lambda_{e_a}^{\alpha_{vis_r}} - n_{dim}\right) + \frac{\lambda_{vis}}{4}\left(J_e^2 - 1 - 2\,\ln J_e\right) - \sum_{r=1}^{n} \mu_{vis_r}\,\ln J_e
\end{aligned} \tag{29}$$

with the Lamé-parameters μ_r, λ and the degree of the polynom α_r for the elastic part as well as with μ_{vis_r}, λ_{vis} and α_{vis_r} for the viscous part. The summation index is given by the parameter r. With an increasing parameter r the complexity of the mapped curve increases. The scalar J is equivalent to the Jacobian determinant of $\mathcal{C}$ and analogously J_e is equal to the Jacobian determinant $\mathcal{C}_e$.

The derivatives of the free energy function ψ with respect to the principal stretches λ_a are called the principal first Piola-Kirchhoff stresses $P_a = \frac{\partial \psi}{\partial \lambda_a}$. For the elastic and the viscous part one gets:

$$\begin{aligned}
P_{ela_a} &= \sum_{r=1}^{n} \mu_r\,\lambda_a^{\alpha_r - 1} - \sum_{r=1}^{n} \mu_r\,\frac{1}{\lambda_a} + \frac{\lambda}{2\,\lambda_a}\left(J^2 - 1\right) \\
P_{vis_a} &= \sum_{r=1}^{n} \mu_{vis_r}\,\lambda_{e_a}^{\alpha_{vis_r} - 1} - \sum_{r=1}^{n} \mu_{vis_r}\,\frac{1}{\lambda_{e_a}} + \frac{\lambda_{vis}}{2\,\lambda_{e_a}}\left(J_e^2 - 1\right)
\end{aligned} \tag{30}$$

The principal second Piola-Kirchhoff stresses are given by $S_a = \frac{1}{\lambda_a}\frac{\partial \psi}{\partial \lambda_a}$. The parameters of the Ogden material model correlate with the linear theory according to [15]:

$$\mu = \frac{1}{2}\sum_{r=1}^{n} \alpha_r\,\mu_r \tag{31}$$

3.2 Derivatives of the free energy function

By means of the principal first Piola-Kirchhoff stresses P_a of Eq. (30) and the definitions of the principal stretches with respect to to the right Cauchy-Green strain tensor of the Subsection 2.3 we get the derivatives

$$\begin{aligned} \frac{\partial \psi_{ela}(\lambda_a)}{\partial \mathcal{C}} &= \sum_{a=1}^{n_{dim}} \frac{\partial \psi_{ela}(\lambda_a)}{\partial \lambda_a} \frac{\partial \lambda_a}{\partial \mathcal{C}} \\ \frac{\partial \psi_{vis}(\lambda_{e_a})}{\partial \mathcal{C}_e} &= \sum_{a=1}^{n_{dim}} \frac{\partial \psi_{vis}(\lambda_{e_a})}{\partial \lambda_{e_a}} \frac{\partial \lambda_{e_a}}{\partial \mathcal{C}_e} \end{aligned} \tag{32}$$

The derivatives of the viscous free energy part with respect to to the variables $\mathcal{C}$ and $\mathcal{U}_i$ are necessary as well:

$$\frac{\partial \psi_{vis}}{\partial \mathcal{C}} = \mathcal{U}_i^{-1} \frac{\partial \psi_{vis}}{\partial \mathcal{C}_e} \mathcal{U}_i^{-1} \qquad \frac{\partial \psi_{vis}}{\partial \mathcal{U}_i} = -2\, \mathcal{U}_i^{-1} \frac{\partial \psi_{vis}}{\partial \mathcal{C}_e} : \mathbb{I}^{sym} \tag{33}$$

4 BALANCES

There exist five balance laws, which are interesting for a dissipative system. These are the balance of mass, the balance of linear momentum, the balance of angular momentum, the first law of thermodynamics and the balance of entropy, see [18].

4.1 Balance of mass

The system we are looking at is a closed system. No mass passes the system, only energy transport is allowed. The mass is constant during the whole motion of the continuum. This can be expressed by:

$$m = \int_{\mathcal{B}_t} \rho(\mathbf{x},\, t)\; \mathrm{d}\, v = \int_{\mathcal{B}_0} \rho_0(\mathbf{X})\; \mathrm{d}\, V = M = \mathrm{const}\,. \tag{34}$$

The mass m of the current configuration must be equal to the mass M of the reference configuration. The deformation of the continuum causes merely a change in the volumn v and the density ρ.

4.2 Balance of linear momentum

The balance of linear momentum is defined as:

$$\frac{\mathrm{d}}{\mathrm{d}\, t}\, \mathbf{J} = \mathbf{f} \tag{35}$$

The time derivative of the linear momentum $\mathbf{J}$ has to be equal to the external forces $\mathbf{f}$. These magnitudes are evaluated by integration over the whole domain $\mathcal{B}_0$:

$$\begin{aligned} \mathbf{J} &= \int_{\mathcal{B}_0} \mathbf{V}\, \rho_0\, \mathrm{d}\, V \\ \mathbf{f} &= \int_{\mathcal{B}_0} \mathbf{b}_0\, \mathrm{d}\, M + \int_{\partial \mathcal{B}_0} \mathbf{t}_0\, \mathrm{d}\, A \end{aligned} \tag{36}$$

By transforming of the surface integrales into volume integrals, we get the global form of the linear momentum theorem:

$$\int_{\mathcal{B}_0} \left(\dot{\mathbf{V}} \, \rho_0 - \mathbf{b}_0 \, \rho_0 - \operatorname{div} \mathcal{P} \right) \mathrm{d}\, V = 0 \tag{37}$$

Thereby merely the mass forces $\mathbf{b}_0$ (in $\mathcal{B}_0$) and the surface forces $\mathbf{t}_0$ (in $\partial\mathcal{B}_0$) are considered. The surface forces lead to the first Piola-Kirchhoff stress tensor $\mathcal{P}$ which correlates with the second Piola-Kirchhoff stress tensor

$$\mathcal{S} = 2 \, \frac{\partial \, \psi(\lambda_a, \lambda_{e_a})}{\partial \mathcal{C}} \tag{38}$$

through the relation

$$\mathcal{S} = \mathcal{F}^{-1} \, \mathcal{P} \tag{39}$$

The velocity $\mathbf{V}$ equals the current velocity $\mathbf{v}$ in value and direction and therewith the time derivative of the current configuration vector $\mathbf{x}$.

If the external forces $\mathbf{f}$ are zero, it can be shown, that the time derivative of the linear momentum is zero. This yields a constant linear momentum:

$$\dot{\mathbf{J}} = \mathbf{0} \qquad \rightarrow \qquad \mathbf{J} = \mathrm{const} \, . \tag{40}$$

4.3 Balance of angular momentum

The balance of angular momentum reads

$$\frac{\mathrm{d}}{\mathrm{d}\, t} \mathbf{L} = \mathbf{m} \tag{41}$$

by the angular momentum $\mathbf{L}$ and the external momentums $\mathbf{m}$. Both can be described in the Lagrangian description:

$$\begin{aligned} \mathbf{L} &= \int_{\mathcal{B}_0} \mathbf{R} \times \mathbf{V} \, \rho_0 \, \mathrm{d}\, V \\ \mathbf{m} &= \int_{\mathcal{B}_0} \mathbf{R} \times \mathbf{b}_0 \, \mathrm{d}\, M + \int_{\partial\mathcal{B}_0} \mathbf{R} \times \mathbf{t}_0 \, \mathrm{d}\, A \end{aligned} \tag{42}$$

whereby $\mathbf{R}$ defines the distance between an arbitrary point $\mathbf{x}_0$ and the point $\mathbf{x}$ at the evaluation of the angular momentum. The conversion of the surface integral into a volume integral with the Gauss' divergence theorem results in the global angular momentum balance:

$$\int_{\mathcal{B}_0} \mathbf{R} \times \left(\dot{\mathbf{V}} \, \rho_0 - \mathbf{b}_0 \, \rho_0 - \operatorname{div} \mathcal{P} \right) \mathrm{d}\, V = 0 \tag{43}$$

The balance of angular momentum leads to similar results like the linear momentum if the external momentums are zero:

$$\dot{\mathbf{L}} = \mathbf{0} \qquad \rightarrow \qquad \mathbf{L} = \mathrm{const} \, . \tag{44}$$

4.4 First law of thermodynamics

The first law of thermodynamics yields the following expression:

$$\dot{H} = -D_{tot}^{int} \tag{45}$$

with the internal dissipation $D_{tot}^{int} = \int_{\mathcal{B}_0} D^{int} \, \mathrm{d}\, V$, which is specified in the next subsection. The total energy H is split into the kinetic energy T and the potential energy V^{int} if one neglects conservative external forces:

$$H = T + V^{int} \tag{46}$$

The kinetic energy T depends on the reference density ρ_0 and the velocity $\mathbf{V}$. The potential energy V^{int} can be derived from the free energy function ψ:

$$\begin{aligned} T &= \frac{1}{2} \int_{\mathcal{B}_0} \rho_0 \, ||\mathbf{V}||^2 \, \mathrm{d}\, V \\ V^{int} &= \int_{\mathcal{B}_0} \psi(\lambda_a, \, \lambda_{e_a}) \, \mathrm{d}\, V \end{aligned} \tag{47}$$

4.5 Balance of entropy

The local balance of entropy, leading to the dissipation D^{int} of the system, is written as:

$$-\dot{\psi} + \frac{1}{2} \mathcal{S} : \dot{\mathcal{C}} \geq 0 \tag{48}$$

for isothermal processes. Employing Eq. (27) in the local balance of entropy, we get:

$$-\frac{\partial \psi}{\partial \mathcal{C}} : \dot{\mathcal{C}} - \frac{\partial \psi_{vis}}{\partial \mathcal{U}_i} : \dot{\mathcal{U}}_i + \frac{1}{2} \mathcal{S} : \dot{\mathcal{C}} \quad \geq 0 \tag{49}$$

The definition of the second Piola-Kirchhoff stress tensor $\mathcal{S}$ of Eq. (38) leads to

$$-\frac{\partial \psi_{vis}}{\partial \mathcal{U}_i} : \dot{\mathcal{U}}_i \geq 0 \tag{50}$$

which defines the non-negative internal dissipation

$$D^{int} := -\frac{\partial \psi_{vis}}{\partial \mathcal{U}_i} : \dot{\mathcal{U}}_i \tag{51}$$

The internal dissipation can be rewritten by the viscous Mandel stress tensor Σ_{vis} and the internal stretch velocity tensor $\mathcal{L}_i^u$:

$$D^{int} = \Sigma_{vis} : \mathcal{L}_i^u \tag{52}$$

with:

$$\Sigma_{vis} = 2 \, \mathcal{C} \frac{\partial \psi_{vis}}{\partial \mathcal{C}} \qquad\qquad \mathcal{L}_i^u = \mathcal{U}_i^{-1} \, \dot{\mathcal{U}}_i \tag{53}$$

5 VISCOSITY

For the characterisation of the evolution equation, we need an isotropic fourth order tensor. This tensor is deduced from the fourth order elasticity tensor $\mathbb{E}$. For this reason it is called the viscosity tensor $\mathbb{V}$. According to [19] the elasticity tensor is split for rubberlike material in an volumetric and a deviatoric part, since these materials have great differences in bulk and shear. We obtain

$$\mathbb{E} = 2\,E_{dev}\,\mathbb{I}^{dev} + E_{vol}\,n_{dim}\,\mathbb{I}^{vol} \tag{54}$$

with the deviatoric and volumetric tensors

$$\mathbb{I}^{dev} = \mathbb{I}^{sym} - \mathbb{I}^{vol} \qquad\qquad \mathbb{I}^{vol} = \frac{1}{n_{dim}}\,I \otimes I \tag{55}$$

The elastic parameters $E_{dev} = \mu$ and $E_{vol} = K$ are given by the well-known Lamé-parameters $\mu,\ \lambda$, and with the bulk modulus K:

$$\lambda = K - \frac{2}{n_{dim}}\,\mu \tag{56}$$

This notation is transfered to the viscoelasticity, according to [8]. The fourth order viscosity tensor $\mathbb{V}$ with the parameters V_{dev} and V_{vol} follows:

$$\mathbb{V} = 2\,V_{dev}\,\mathbb{I}^{dev} + V_{vol}\,n_{dim}\,\mathbb{I}^{vol} \tag{57}$$

With the symmetric internal variable and $\lambda_{vis},\ K_{vis},\ \mu_{vis} > 0$ to describe the non-negativ dissipation, we have only two restrictions. The symmetric unit tensor $\mathbb{I}^{sym}$ of deviatoric tensor $\mathbb{I}^{dev}$ has to be changed in $\mathbb{I}^{\mathrm{T}} = \delta_{il}\,\delta_{jk}$:

$$\mathbb{I}^{dev} \;=\; \mathbb{I}^{\mathrm{T}} - \mathbb{I}^{vol} \tag{58}$$

and the parameters are restricted in the following way:

$$V_{dev} > 0 \qquad\qquad V_{vol} > \frac{2\,V_{dev}}{n_{dim}} \tag{59}$$

These guidlines lead to the dissipation:

$$\mathcal{L}_i^u : \mathbb{V} : \mathcal{L}_i^u \geq 0 \tag{60}$$

with:

$$\Sigma_{vis} = \mathbb{V} : \mathcal{L}_i^u \tag{61}$$

6 SPATIAL DISCRETISATION

For the spatial discretisation EAS elements are used, which exhibit enhanced degrees of freedom. The reason is that the well-known nonlinear standard displacement based elements lead to locking effects in combination with high Poissons numbers and high dominance of bending. This causes a non-physical stiffening of the body.

A remedy could be an underintegration of the Gaussian integration. But this yields in many cases hourglass effects, which are characterised by non-physical deformations. The best possibility to remedy these locking effects is the EAS element, according to [11]. This element can model large strain for elastic materials as well as for inelastic materials, see also [20].

6.1 Isoparametric concept

The spatial discretisation is done in conjunction with the isoparametric concept. Therefore the physical fields (positions $\mathbf{q}$, $\mathbf{q}_\alpha$ and the velocities $\mathbf{v}$) and the geometry ($\mathbf{q}_0$) are approximated with the same global shape functions $N_I(\mathbf{X})$ and $M_I(\mathbf{X})$, respectively.

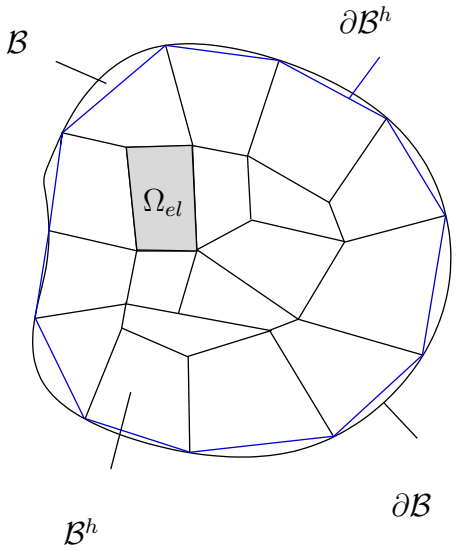

Figure 2: Approximation of the domain $\mathcal{B}$.

The domain $\mathcal{B}$ as well as the boundary of the domain $\partial\mathcal{B}$ are approximated by the sets $\mathcal{B}^h$ and $\partial\mathcal{B}^h$, as shown in Figure 2:

$$\mathcal{B} \approx \mathcal{B}^h = \bigcup_{el=1}^{n_{el}} \Omega_{el} \qquad \partial\mathcal{B} \approx \partial\mathcal{B}^h = \bigcup_{el=1}^{n_{be}} \partial\Omega_{el} \tag{62}$$

with the elements Ω_{el} and the boundary elements $\partial\Omega_{el}$, respectively and the number of elements n_{el} and the boundary elements n_{be}, respectively.

The configuration vector $\mathbf{q}$, the linear momentum $\mathbf{p}$ and the enhanced degrees of freedom $\mathbf{q}_\alpha$ of each element are now discretised with the shape functions $N_I(\mathbf{X})$ and $M_I(\mathbf{X})$, respectively. The approximation is as follows:

$$\begin{aligned}
\mathbf{q} &\approx \mathbf{q}_{el} = \sum_{n=1}^{n_{node}} N_I\, \mathbf{q}_I \\
\mathbf{p} &\approx \mathbf{p}_{el} = \sum_{n=1}^{n_{node}} N_I\, \mathbf{p}_I \\
\mathbf{q}_\alpha &\approx \mathbf{q}_{\alpha_{el}} = \sum_{n=1}^{n_{enh}} M_I\, \mathbf{q}_{\alpha_I}
\end{aligned} \tag{63}$$

with the nodes per element $n_{node} = 4$ and the enhanced nodes $n_{enh} = 2$. The shape functions

N_I of the four node element, given by

$$N_1(\boldsymbol{\xi}) = \frac{1}{4}(1-\xi)(1-\eta) \qquad N_3(\boldsymbol{\xi}) = \frac{1}{4}(1+\xi)(1+\eta)$$
$$N_2(\boldsymbol{\xi}) = \frac{1}{4}(1+\xi)(1-\eta) \qquad N_4(\boldsymbol{\xi}) = \frac{1}{4}(1-\xi)(1+\eta) \tag{64}$$

and the bubble modes M_I for the enhanced nodes, defined by

$$M_1 = 1-\xi^2 \qquad M_2 = 1-\eta^2 \tag{65}$$

depend on the coordinates ξ and η of the master element $\Omega_\square = [-1,\,1]\times[-1,\,1]$. This correlation is depicted in Figure 3. The master element $\Omega_\square$ can describe an element of the reference configuration in the domain $\mathcal{B}_0$ or an element of the current configuration in the domain $\mathcal{B}_t$.

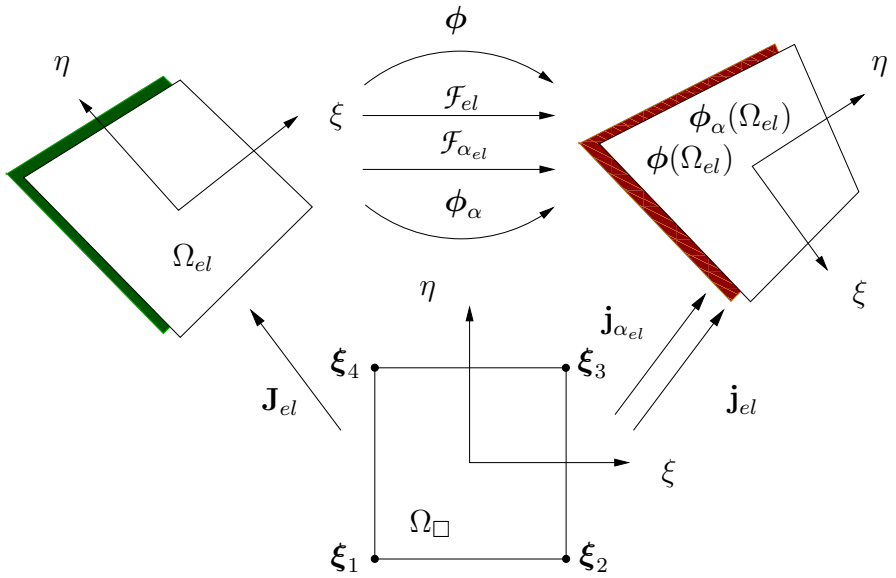

Figure 3: Isoparametric transformation of the deformation of an element.

The reference configuration $\mathbf{X}$ ($\hat{=}\,\mathbf{q}_{0_{el}}$) can be interpolated analogously to the current configuration $\mathbf{x}$ ($\hat{=}\,\mathbf{q}_{el}$) from Eq. 63_1 with:

$$\mathbf{q}_{0_{el}} = \sum_{n=1}^{n_{node}} N_I(\boldsymbol{\xi})\,\mathbf{q}_{0_I} \tag{66}$$

The transformation of the tangent space is given by the gradients $\mathbf{J}_{el}$ and $\mathbf{j}_{el}$. The transformation for the enhanced degrees of freedom $\mathbf{q}_{\alpha_{el}}$ leads to a gradient $\mathbf{j}_{\alpha_{el}}$:

$$\mathbf{j}_{el} = \frac{\partial\,\mathbf{q}_{el}}{\partial\,\boldsymbol{\xi}} = \sum_{I=1}^{n} \mathbf{q}_I \otimes \nabla_\xi N_I(\boldsymbol{\xi}) \tag{67}$$
$$\mathbf{J}_{el} = \frac{\partial\,\mathbf{q}_{0_{el}}}{\partial\,\boldsymbol{\xi}} = \sum_{I=1}^{n} \mathbf{q}_{0_I} \otimes \nabla_\xi N_I(\boldsymbol{\xi})$$
$$\mathbf{j}_{\alpha_{el}} = \frac{\partial\,\mathbf{q}_{\alpha_{el}}}{\partial\,\boldsymbol{\xi}} = \sum_{I=1}^{n} \mathbf{q}_{\alpha_I} \otimes \nabla_\xi M_I(\boldsymbol{\xi})$$

The deformation gradients $\mathcal{F}_{el}$ and the gradient of the enhanced degrees of freedom $\mathcal{F}_{\alpha_{el}}$ can be described with the gradients of Eq. (67):

$$\mathcal{F}_{el} = \frac{\partial\, \mathbf{q}_{el}}{\partial\, \mathbf{q}_{0_{el}}} = \mathbf{j}_{el}\, \mathbf{J}_{el}^{-1} \qquad \mathcal{F}_{\alpha_{el}} = \frac{\partial\, \mathbf{q}_{\alpha_{el}}}{\partial\, \mathbf{q}_{0_{el}}} = \mathbf{j}_{\alpha_{el}}\, \mathbf{J}_{el}^{-1} \tag{68}$$

After these evaluations we get the right Cauchy-Green strain tensor $\mathcal{C}_{el}^{enh}$ for each element:

$$\begin{aligned} \mathcal{C}_{el}^{enh} &= \mathcal{F}_{el}^{enh\,\mathrm{T}}\, \mathcal{F}_{el}^{enh} \\ &= (\mathcal{F}_{el} + \mathcal{F}_{\alpha_{el}})^{\mathrm{T}}\, (\mathcal{F}_{el} + \mathcal{F}_{\alpha_{el}}) \end{aligned} \tag{69}$$

The remaining quantities can be derived analogously for each element.

6.2 Gaussian integration

The volume integrals, as the integrals of Eq. (47), for instance, have to be integrated numerically. This is done by the Gaussian integration. The integral over the domain $\mathcal{B}_0$ can be expressed by the master element $\Omega_\square$:

$$\int_{\mathcal{B}_0} g(\mathbf{X})\, \mathrm{d}\, V = \bigcup_{el=1}^{n_{el}} \int_{\Omega_{el}} g(\mathbf{X})\, \mathrm{d}\, \Omega_{el} = \bigcup_{el=1}^{n_{el}} \int_{\Omega_\square} g(\boldsymbol{\xi})\, \det \mathbf{J}_{el}\, \mathrm{d}\, \Omega_\square \tag{70}$$

Whereby the integration over the boundaries of the masterelement $\Omega_\square$ leads to:

$$\int_{-1}^{1} \int_{-1}^{1} g(\xi,\, \eta)\, \det \mathbf{J}_{el}\, \mathrm{d}\, \xi\, \mathrm{d}\, \eta \approx \sum_{p=1}^{n_p} g(\xi_p,\, \eta_p) \det \mathbf{J}_{el}(\xi_p,\, \eta_p)\, W_p \tag{71}$$

with the weighting factors W_p and the integration points $(\xi_p,\, \eta_p)$ with the number $n+1$ per dimension. The degree of accuracy m coincides with $2\,n+1$. The following integrals are of size $m \leqslant 3$. Therfore we choose $n = 1$ and obtain $n_p = 4$. The weighting factors are then $W_1 = W_2 = W_3 = W_4 = 1$ with the integration points

$$\begin{aligned} \boldsymbol{\xi}_1 &= (-\frac{1}{\sqrt{3}},\, -\frac{1}{\sqrt{3}}) \qquad \boldsymbol{\xi}_2 = (\ \ \frac{1}{\sqrt{3}},\, -\frac{1}{\sqrt{3}}) \\ \boldsymbol{\xi}_3 &= (\ \ \frac{1}{\sqrt{3}},\ \ \frac{1}{\sqrt{3}}) \qquad \boldsymbol{\xi}_4 = (-\frac{1}{\sqrt{3}},\ \ \frac{1}{\sqrt{3}}) \end{aligned} \tag{72}$$

7 SEMIDISCRETE HAMILTON'S EQUATIONS

7.1 Hamilton's formulation

The Hamilton function H is given by the Legendre transformation of the Lagrange function $L = T + V^{int}$ by means of the linear momentum

$$\mathbf{p} = \frac{\partial L}{\partial\, \dot{\mathbf{q}}} = \mathbf{M}\, \dot{\mathbf{q}} \tag{73}$$

as new variable. The Hamilton function then reads:

$$H = T + V^{int} \tag{74}$$

where T denotes the kinetic energy

$$T = \frac{1}{2} \int_{\mathcal{B}_0} \mathbf{p}\, \mathbf{M}^{-1}\, \mathbf{p}\; \mathrm{d}\, V \tag{75}$$

The derivatives of the total energy H with respect to both variables $\mathbf{q}$ and $\mathbf{p}$ lead to the semidiscrete Hamiltons equation:

$$\begin{aligned} \dot{\mathbf{q}} &= \nabla_{\mathbf{p}} H \quad = \mathbf{M}^{-1}\, \mathbf{p} \\ \dot{\mathbf{p}} &= -\nabla_{\mathbf{q}} H = -\mathbf{F}^{int} \end{aligned} \tag{76}$$

The internal forces $\mathbf{F}^{int}$ can be derived from the internal potential energy V^{int}:

$$\mathbf{F}^{int} = \int_{\mathcal{B}_0} \frac{\partial \psi(\lambda_a,\, \lambda_{e_a})}{\partial \mathcal{C}} : \frac{\partial \mathcal{C}}{\partial\, \mathbf{q}}\, \mathrm{d}\, V \tag{77}$$

7.2 Hamilton's formulation with enhanced degrees of freedom

According to [11] there corresponds a third equation to the enhanced degrees of freedom. This third equation is given by the Hu-Washizu functional Π, which describes the total potential for elastic or inelastic materials

$$\Pi = \int_{\mathcal{B}_0} \psi - \mathcal{P} : \mathcal{F}_\alpha\, \mathrm{d}\, V \tag{78}$$

This potential defines the configuration $\boldsymbol{\phi}$, the deformation tensor $\mathcal{F}_\alpha$ and the first Piola-Kirchhoff stress tensor $\mathcal{P}$ as independent variables. Applying standard procedures from the calculus of variations yields the governing equations:

$$\begin{aligned} \dot{\mathbf{q}} &= \mathbf{M}^{-1}\, \mathbf{p} \\ \dot{\mathbf{p}} &= -\mathbf{F}^{int} \\ \mathbf{0} &= \mathbf{S}^{int} \end{aligned} \tag{79}$$

The internal forces $\mathbf{F}^{int}$ and the enhanced internal forces $\mathbf{S}^{int}$ are given by:

$$\begin{aligned} \mathbf{F}^{int} &= \int_{\mathcal{B}_0} \frac{\partial \psi(\lambda_a^{enh},\, \lambda_{e_a}^{enh})}{\partial \mathcal{C}^{enh}} : \frac{\partial \mathcal{C}^{enh}}{\partial\, \mathbf{q}}\, \mathrm{d}\, V \\ \mathbf{S}^{int} &= \int_{\mathcal{B}_0} \frac{\partial \psi(\lambda_a^{enh},\, \lambda_{e_a}^{enh})}{\partial \mathcal{C}^{enh}} : \frac{\partial \mathcal{C}^{enh}}{\partial\, \mathbf{q}_\alpha}\, \mathrm{d}\, V \end{aligned} \tag{80}$$

7.3 Evolution equation

The internal variable $\mathcal{U}_i$ leads to an additional equation, which is called the evolution equation. This equation is given by Eq. (61). With Eq. $(53)_1$ and Eq. (33) we get:

$$\begin{aligned} \Sigma_{vis} &= \mathbb{V} : \mathcal{L}_i^u \\ 2\, \mathcal{C}\, \mathcal{U}_i^{-1}\, \frac{\partial\, \psi_{vis}}{\partial \mathcal{C}_e}\, \mathcal{U}_i^{-1} &= \mathbb{V} : \mathcal{L}_i^u \\ -\frac{\partial\, \psi_{vis}}{\partial\, \mathcal{U}_i} &= \mathcal{U}_i^{-1}\, [\mathbb{V} : \mathcal{L}_i^u] \end{aligned} \tag{81}$$

The rate $\dot{\mathcal{U}}_i$ of the viscous stretch tensor is included in the viscous velocity tensor $\mathcal{L}_i^u$ (see Eq. $(53)_2$). There is no reason to convert the last equation into the form $\dot{\mathcal{U}}_i = f(\mathcal{C}, \mathcal{U}_i)$. So the evolution equation is given by:

$$-\frac{\partial \psi_{vis}}{\partial \mathcal{U}_i} = \mathcal{U}_i^{-1}\,[\mathbb{V} : \mathcal{U}_i^{-1}\,\dot{\mathcal{U}}_i] \tag{82}$$

8 TIME DISCRETISATION

The time discretisation has to be consistent with the balance laws introduced in Section 4. For the algorithmic conservation properties we need a common integration rule, which is specified step by step (compare [9]). The algorithmic properties are the conservation of linear momentum and angular momentum and the satisfaction of the energy balance.

8.1 Time integration

The time axis t is divided in equidistant time intervals $T_n = [t_n,\, t_{n+1}]$ with the interval length $\Delta t = t_{n+1} - t_n$ for a common time integration. Furthermore we introduce a variable α, which maps the time interval T_n to an unit interval $[0,\, 1]$:

$$\alpha = \frac{t - t_n}{t_{n+1} - t_n} = \frac{t - t_n}{\Delta t} \tag{83}$$

The derivative of the variable α with respect to time t leads to the differential relation

$$\mathrm{d}\,t = \Delta t\;\mathrm{d}\,\alpha \tag{84}$$

The linear approximation of an arbitrary quantity $\circ$ which depends on α and the derivative with respect to the variable α are given as follows:

$$\begin{aligned} \circ\,(\alpha) &\equiv \circ_{n+\alpha} = (1-\alpha)\;\circ_n + \alpha\;\circ_{n+1} \\ \frac{\mathrm{d}\,\circ(\alpha)}{\mathrm{d}\,\alpha} &= \circ_{n+1} - \circ_n = \Delta\circ \end{aligned} \tag{85}$$

Eq. (79) can than be described by:

$$\mathbf{q}_{n+1} - \mathbf{q}_n = \Delta t\,\mathbf{M}^{-1} \int_0^1 \mathbf{p}_{n+\alpha}\;\mathrm{d}\,\alpha \tag{86}$$

$$\mathbf{p}_{n+1} - \mathbf{p}_n = -\Delta t \int_0^1 \mathbf{F}^{int}_{n+\alpha}\;\mathrm{d}\,\alpha$$

$$\mathbf{0} = \Delta t \int_0^1 \mathbf{S}^{int}_{n+\alpha}\;\mathrm{d}\,\alpha$$

8.2 Algorithmic conservation of linear momentum

The algorithmic balance of linear momentum is fulfilled if

$$\mathbf{J}_{n+1} - \mathbf{J}_n = \mathbf{0} \tag{87}$$

It can be easily shown, that this balance is satisfied for any consistent time-stepping scheme.

8.3 Algorithmic conservation of angular momentum

The algorithmic balance of angular momentum

$$\mathbf{L}_{n+1} - \mathbf{L}_n = \mathbf{0} \tag{88}$$

is only fulfilled by setting $\alpha = \frac{1}{2}$. This coincides with the midpoint rule for the time discretisation.

8.4 Algorithmic fulfillment of the balance of energy

For the algorithmic satisfaction of the balance of energy we enforce the following equation:

$$H_{n+1} - H_n = -D_{tot}^{int} \tag{89}$$

The fundamental theorem of integral calculus yields:

$$\begin{aligned} H_{n+1} - H_n &= \int_0^1 \frac{\mathrm{d}\, H_{n+\alpha}}{\mathrm{d}\,\alpha}\, \mathrm{d}\,\alpha \qquad (90) \\ (T_{n+1} - T_n) + (V_{n+1}^{int} - V_n^{int}) &= \int_0^1 \left(\frac{\mathrm{d}\, T_{n+\alpha}}{\mathrm{d}\,\alpha} + \frac{\mathrm{d}\, V_{n+\alpha}^{int}}{\mathrm{d}\,\alpha} \right) \mathrm{d}\,\alpha \end{aligned}$$

It can be shown, that the kinetic energy can be integrated exactly with the midpoint rule ($\alpha = \frac{1}{2}$). With this in mind there remains only the fundamental theorem of integral calculus for the potential energy V^{int}:

$$V_{n+1}^{int} - V_n^{int} = \int_0^1 \int_{\mathcal{B}_0} \frac{\mathrm{d}\, \psi_{n+\alpha}(\lambda_a^{enh},\, \lambda_{e_a}^{enh})}{\mathrm{d}\,\alpha}\, \mathrm{d}\, V\, \mathrm{d}\,\alpha \tag{91}$$

A further split leads to an equation, which has to be fulfilled in each element:

$$\psi_{n+1} - \psi_n - \int_0^1 \left(\frac{\partial\, \psi_{n+\alpha}(\lambda_a^{enh},\, \lambda_{e_a}^{enh})}{\partial \mathcal{C}^{enh}} : \frac{\partial \mathcal{C}^{enh}}{\partial \alpha} + \frac{\partial\, \psi_{n+\alpha}(\lambda_a^{enh},\, \lambda_{e_a}^{enh})}{\partial \mathcal{C}_i} : \frac{\partial \mathcal{C}_i}{\partial \alpha} \right) \mathrm{d}\,\alpha = 0 \tag{92}$$

Now we have to minimise the functional G, which relies on additional stresses $\tilde{\mathcal{S}}$:

$$G(\tilde{\mathcal{S}},\, \lambda) = F(\tilde{\mathcal{S}}) + \lambda\, E(\tilde{\mathcal{S}}) \tag{93}$$

with the minimisation functional

$$F(\tilde{\mathcal{S}}) = \frac{1}{2}\, ||\tilde{\mathcal{S}}||^2 = \frac{1}{2}\, \tilde{\mathcal{S}} : \tilde{\mathcal{S}} \tag{94}$$

and the constraint

$$E(\tilde{\mathcal{S}}) = \psi_{n+1} - \psi_n - \int_0^1 \left(\frac{1}{2}\, [\mathcal{S}^{enh} + \tilde{\mathcal{S}}] : \frac{\partial \mathcal{C}^{enh}}{\partial \alpha} + \frac{\partial\, \psi_{n+\alpha}}{\partial \mathcal{C}_i} : \frac{\partial \mathcal{C}_i}{\partial \alpha} \right) \mathrm{d}\,\alpha = 0 \tag{95}$$

The conditions $\frac{\partial G}{\partial \tilde{\mathcal{S}}} = \boldsymbol{0}$ and $\frac{\partial G}{\partial \lambda} = 0$ lead to the discrete gradient

$$\bar{\nabla}\psi = \left(\frac{\partial\, \psi}{\partial \mathcal{C}^{enh}} \right)_{n+\frac{1}{2}} + \frac{\psi_{n+1} - \psi_n - \left(\frac{\partial\, \psi}{\partial \mathcal{U}_i} \right)_{n+\frac{1}{2}} : \Delta \mathcal{U}_i - \left(\frac{\partial\, \psi}{\partial \mathcal{C}^{enh}} \right)_{n+\frac{1}{2}} : \Delta \mathcal{C}^{enh}}{||\Delta \mathcal{C}^{enh}||^2}\, \Delta \mathcal{C}^{enh} \tag{96}$$

The index $n + \frac{1}{2}$ implies the evaluation at the midpoint of the strains.

9 TIME DISCRETE EQUATIONS

The time discretisation with the discrete gradient of Eq. (96) yields an energy consistent scheme. The discrete Hamilton's equation are given by:

$$\begin{aligned} \mathbf{q}_{n+1} - \mathbf{q}_n &= \Delta t\, \mathbf{M}^{-1}\, \mathbf{p}_{n+\frac{1}{2}} \\ \mathbf{p}_{n+1} - \mathbf{p}_n &= -\Delta t\, \bar{\mathbf{F}}^{int} \\ \mathbf{0} &= \bar{\mathbf{S}}^{int} \end{aligned} \tag{97}$$

with the discretised internal forces $\bar{\mathbf{F}}^{int}$ and the discretised enhanced internal forces $\bar{\mathbf{S}}^{int}$:

$$\begin{aligned} \bar{\mathbf{F}}^{int} &= \int_{\mathcal{B}_0} \bar{\nabla}\psi : \frac{\partial \mathcal{C}^{enh}\left(\mathbf{q}_{n+\frac{1}{2}},\, \mathbf{q}_{\alpha_{n+\frac{1}{2}}}\right)}{\partial\, \mathbf{q}_{n+\frac{1}{2}}}\, \mathrm{d}\, V \\ \bar{\mathbf{S}}^{int} &= \int_{\mathcal{B}_0} \bar{\nabla}\psi : \frac{\partial \mathcal{C}^{enh}\left(\mathbf{q}_{n+\frac{1}{2}},\, \mathbf{q}_{\alpha_{n+\frac{1}{2}}}\right)}{\partial\, \mathbf{q}_{\alpha_{n+\frac{1}{2}}}}\, \mathrm{d}\, V \end{aligned} \tag{98}$$

The evolution equation is discretised by the ordinary midpoint rule:

$$-\left(\frac{\partial \psi_{vis}}{\partial \mathcal{U}_i}\right)_{n+\frac{1}{2}} - \mathcal{U}^{-1}_{i_{n+\frac{1}{2}}}\, \mathbb{V} : \mathcal{U}^{-1}_{i_{n+\frac{1}{2}}} \left(\frac{\mathcal{U}_{i_{n+1}} - \mathcal{U}_{i_n}}{\Delta t}\right) = 0 \tag{99}$$

10 EXAMPLES

As example we show a two dimensional free flying L with an initial velocity $v_0 = 6$ and an initial angular velocity $\omega = 0.6$, see Figure 4. The spatial discretisation is done by 36 EAS elements. The side length of the free flying L is $l = 10$, so each quadrilateral is of size 1×1 in the initial configuration. The x-y coordinate system is fixed on the edge point in the initial configuration on the symmetry axis of the L. The density ρ_0 is chosen $8,93$ and the time step-size is given by $\Delta t = 0,05$s.

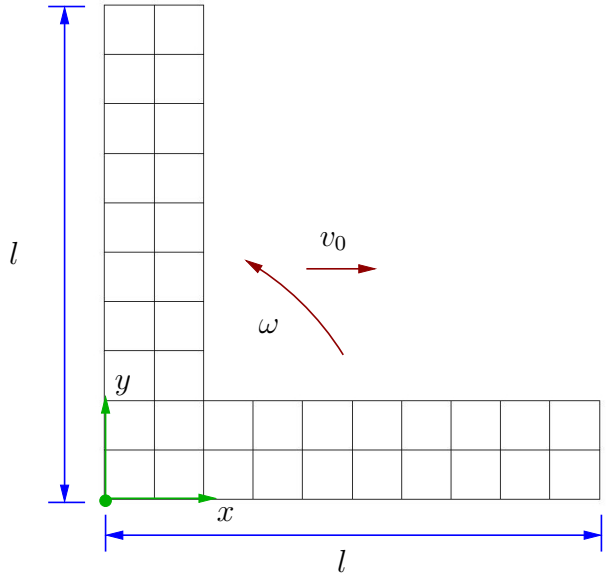

Figure 4: Initial configuration and velocities of the free flying L.

10.1 Large strains

The first motion is the free flying L under large strains. Therefore the Lamé-parameters of the Ogden material model are chosen to obtain a very flexible material response, see Table 1.

elastic			viscous		
Lamé-parameters		polynom	Lamé-parameters		polynom
$\mu_1 = 1026,09$	$\lambda = 3000$	$\alpha_1 = 1,5$	$\mu_{vis_1} = 1026,09$	$\lambda_{vis} = 3000$	$\alpha_{vis_1} = 1,5$
$\mu_2 = -0,78$		$\alpha_2 = -7,5$	$\mu_{vis_2} = -0,78$		$\alpha_{vis_2} = -7,5$
$\mu_3 = 0,17$		$\alpha_3 = 12,0$	$\mu_{vis_3} = 0,17$		$\alpha_{vis_3} = 12,0$

Table 1: Parameters for the soft Ogden material.

The viscosity parameters of the fourth order viscosity tensor $\mathbb{V}$ are $V_{dev} = 10000$ and $V_{vol} = 50000$. The tolerance for the Newton-Raphson iteration is given by $\varepsilon = 10^{-8}$ for the evaluation of the Hamiltons equation and analogously this tolerance is chosen for the iteration of the evolution equation $\varepsilon_{vis} = 10^{-8}$. The simulation runs 20s and the results of the simulation are depicted in the next figures.

The total energy H and the dissipation D_{tot}^{int} are displayed in the Figures 5a and 5b. The total energy H is the whole time of the motion steady decreasing, which is supposed to be for

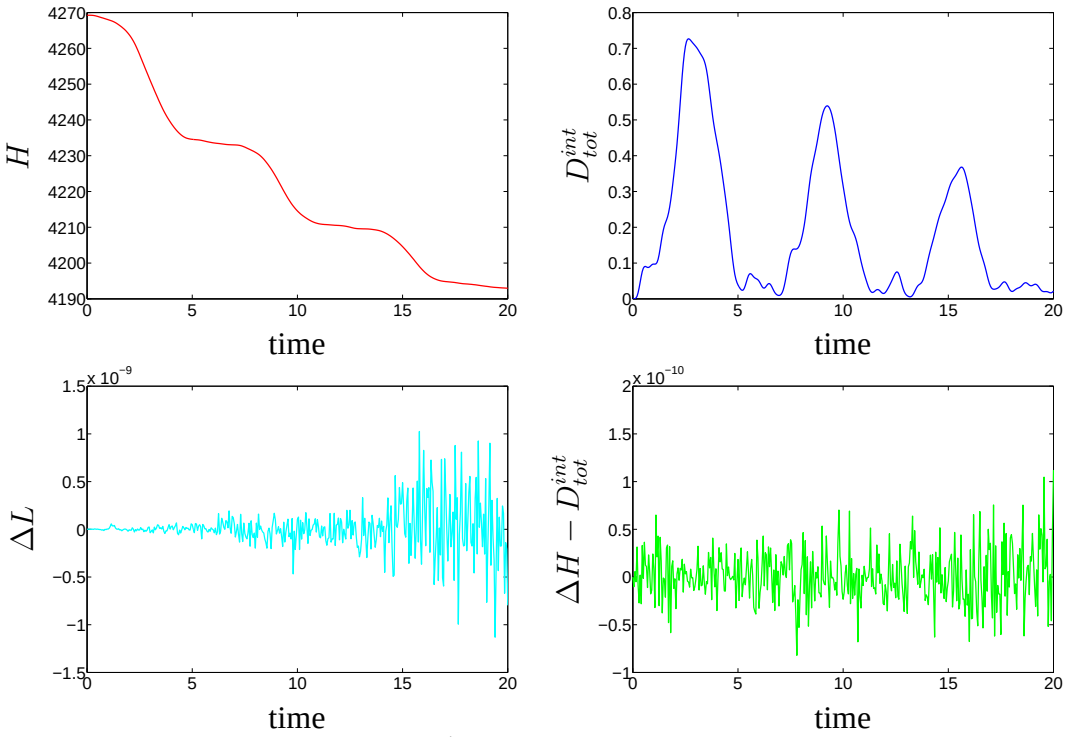

Figure 5: a) Total energy H, b) dissipation D_{tot}^{int}, c) Δ-function of the angular momentum and d) energy balance $\dot{H} - D_{tot}^{int} = 0$ of the free flying L with large strain.

a dissipative material model. The dissipation D^{int} is always non-negative and its amplitude slopes down.

The algorithmic conservation properties are shown for the balance of angular momentum with the ΔL-function, see Figure 5c. This function compares the angular momentum of two successive time steps ($\mathbf{L}_n$, $\mathbf{L}_{n+1}$). The energy balance is given in Figure 5d. Both figures show, that the angular momentum and the energy balance are fulfilled for the underlying tolerance.

The motion of the free flying L is given by the snapshots in Figure 6.

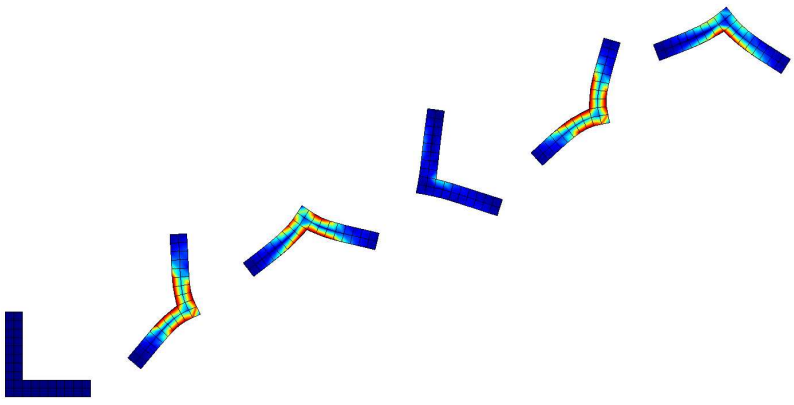

Figure 6: Snapshots of the free flying L at the time steps $t = [0\,4\,8\,12\,16\,20]$s.

The color shows the interpolated norm of the Kirchhoff stresses $||\tau||$.

10.2 Quasi rigid body

The second example is the free flying L perfoming a quasi rigid body motion. This implies very stiff material parameters for the Ogden material model, see Table 2.

elastic			viscous		
Lamé-parameters		polynom	Lamé-parameters		polynom
$\mu_1 = 10260,96$	$\lambda = 30000$	$\alpha_1 = 1,5$	$\mu_{vis_1} = 10260,96$	$\lambda_{vis} = 30000$	$\alpha_{vis_1} = 1,5$
$\mu_2 = -7,78$		$\alpha_2 = -7,5$	$\mu_{vis_2} = -7,78$		$\alpha_{vis_2} = -7,5$
$\mu_3 = 1,70$		$\alpha_3 = 12,0$	$\mu_{vis_3} = 1,70$		$\alpha_{vis_3} = 12,0$

Table 2: Parameters for the higher Ogden material.

The parameters for the viscosity tensor $\mathbb{V}$ have not been changed. The tolerance of the Newton-Raphson iteration for the Hamilton equation and the evolution equation are chosen as $\varepsilon = \varepsilon_{vis} = 10^{-6}$. The simulation runs once again 20s.

The total energy H and the dissipation D_{tot}^{int} are shown in the Figures 7a and 7b. Both figures show the same results as in the aforementioned example. The fast decay of the energy to a constant level and of the dissipation to zero is due to the higher material parameters of the Ogden model.

The algorithmic conservation of angular momentum and the balance of energy are once again fulfilled in the underlying tolerance, see Figure 7c and 7d.

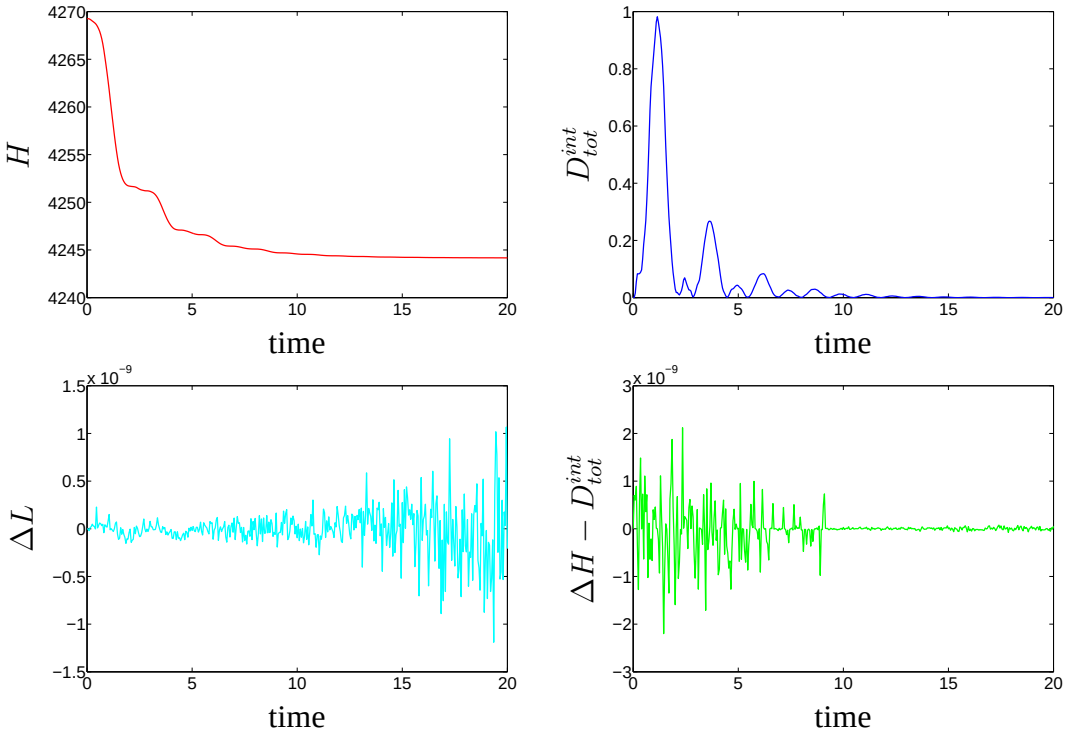

Figure 7: a) Total energy H, b) dissipation D_{tot}^{int}, c) Δ-function of the angular momentum and d) energy balance $\dot{H} - D_{tot}^{int} = 0$ of the free flying L performing a quasi rigid body motion.

The motion of the free flying L perfoming a quasi rigid body motion is given by the snapshots in the Figure 8.

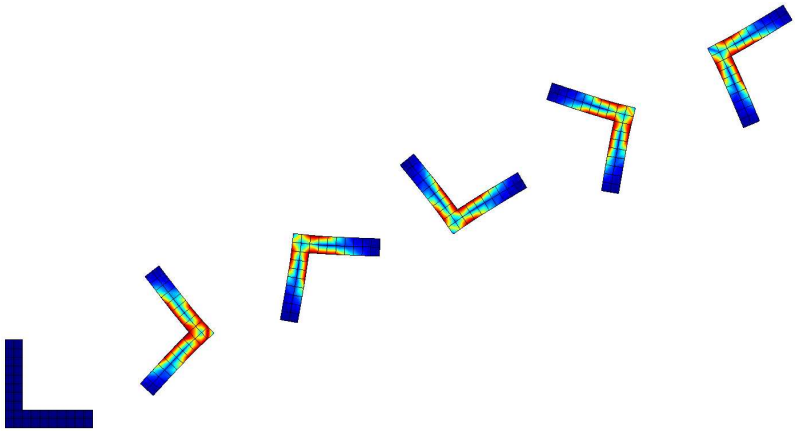

Figure 8: Snapshots of the free flying L at the time steps $t = [0\,4\,8\,12\,16\,20]$s.

The color shows once again the interpolated norm of the Kirchhoff stresses $||\tau||$.

11 CONCLUSIONS

In the presented work we deal with an internal, history dependend variable, which is chosen analogously to the stretch tensor. The used material model is the Ogden material model, which is well-suited for rubberlike materials. Moreover we use enhanced assumed strain elements (EAS) for the discretisation in space and a discrete gradient for the time discretisation.

The internal variable $\mathcal{U}_i$ leads to a symmetric strain measure $\mathcal{C}_e$ for the viscous part of the free energy function ψ. Furthermore the evolution equation is realised with a fourth order viscosity tensor $\mathbb{V}$ which guarantees the positivity of the dissipation and the symmetry of the internal variable.

The EAS elements for the discretisation in space remedy the locking effects of the nonlinear displacement based elements, which occurs for high Poissons numbers in combination with high dominance of bending. This effect occurs very often, since rubberlike materials have Poissons numbers of $\nu \approx 0,5$.

The discretisation in time is done by a discrete gradient, which has to be included in the Hamilton's equation and the equations corresponding to the enhanced degrees of freedom. This leads to a new energy-momentum scheme (EAS-EM method) for viscoelasticity using EAS elements.

This allows us to simulate large strain deformation viscoelasticity and fulfil at the same time the conservation properties. The fulfilled conservation properties lead to an improved numerical stability of the system.

REFERENCES

[1] J.C. Simo, On a fully three-dimensional finite-strain viscoelastic damage model: formulation and computational aspects. *Computer Methods in Applied Mechanics and Engineering*, **60**, 153–173, 1987.

[2] S. Govindjee and J.C. Simo, Mullins's effect and the strain amplitude dependence of the storage modulus. *International Journal of Solids and Structures*, **29**, 1737–1751, 1992.

[3] M. Kaliske, *Zur Theorie und Numerik von Polymerstrukturen unter statischen und dynamischen Einwirkungen*. Dissertation, Mitteilung Nr. 41-95, Institut für Statik. Universität Hannover, 1995.

[4] G.A. Holzapfel, On large strain viscoelasticity: continuum formulation and finite element applications to elastomeric structures. *International Journal for Numerical Methods in Engineering*, **39**, 3903–3926, 1996.

[5] J. Lubliner, A model of rubber viscoelasticity. *Mechanics Research Communications*, **12**, 93–99, 1985.

[6] S. Reese, *Thermomechanische Modellierung gummiartiger Polymerstrukturen*. Habilitationsschrift, F 01/4, Institut für Baumechanik und numerische Mechanik. Universität Hannover, 2000.

[7] C. Miehe, *Kanonische Modelle multiplikativer Elastoplastizität. Thermodynamische Formulierungen und numerische Implementation*. Habilitationsschrift, F 93/1, Institut für Baumechanik und numerische Mechanik. Universität Hannover, 1993.

[8] M. Groß and P. Betsch, Energy-momentum consistent finite element discretisation of dynamic finite deformation viscoelasticity. *submitted for publication.*

[9] P. Betsch and P. Steinmann, Conservation properties of a time FE method-Part II: Time stepping schemes for non-linear elastodynamics. *International Journal for Numerical Methods in Engineering*, **50**, 1931–1955, 2001.

[10] O. Gonzalez, Exact energy and momentum conserving algorithms for general models in nonlinear elasticity. *Computer Methods in Applied Mechanics and Engineering*, **190**, 1763–1783, 2000.

[11] J.C. Simo and F. Armero, Geometrically non-linear enhanced strain mixed methods and the method of incompatible modes. *International Journal for Numerical Methods in Engineering*, **33**, 1413–1449, 1992.

[12] J.C. Simo, F. Armero and R.L. Taylor, Improved versions of assumed enhanced strain tri-linear elements for 3D finite deformation problems. *Computer Methods in Applied Mechanics and Engineering*, **110**, 359–386, 1993.

[13] P. Wriggers and S. Reese, A note on enhanced strain methods for large deformations. *Computer Methods in Applied Mechanics and Engineering*, **135**, 201–209, 1996.

[14] R.W. Ogden, Large deformation isotropic elasticity - on correlation of theory and experiment for incompressible rubberlike solids. *Royal society of London A*, **326**, 565–584, 1972.

[15] R.W. Ogden, Large deformation isotropic elasticity - on correlation of theory and experiment for compressible rubberlike solids. *Royal society of London A*, **328**, 567–583, 1972.

[16] I. Büthe et al. *Polyurethane. Spezialkunststoffe für Industrie und Handwerk - Verarbeitung, Eigenschaften, Anwendung*. Expert Verlag, 1989.

[17] J.C. Simo and R.L. Taylor, Quasi-incompressible finite elasticity in principal stretches. Continuum basis and numerical algorithms. *Computer Methods in Applied Mechanics and Engineering*, **85**, 273–310, 1991.

[18] G.A. Holzapfel, *Nonlinear solid mechanics. A continuum approach for engineering*. John Wiley & Sons Ltd., 2000.

[19] J. Betten, *Kontinuumsmechanik. Elasto-, Plasto-, Kriechmechanik*. Springer-Verlag, 1993.

[20] P. Wriggers, *Nichtlineare Finite-Element-Methoden*. Springer-Verlag, 2001.